A Blood-Based Metabolite Panel for Distinguishing Ovarian Cancer from Benign Pelvic Masses

Ehsan Irajizad[1], Chae Y. Han[2], Joseph Celestino[2], Ranran Wu[3], Eunice Murage[3], Rachelle Spencer[3], Jennifer B. Dennison[3], Jody Vykoukal[3], James P. Long[1], Kim Anh Do[1], Charles Drescher[4,5], Karen Lu[6], Zhen Lu[6], Robert C. Bast[6], Sam Hanash[3], and Johannes F. Fahrmann[3]

ABSTRACT

Purpose: To assess the contributions of circulating metabolites for improving upon the performance of the risk of ovarian malignancy algorithm (ROMA) for risk prediction of ovarian cancer among women with ovarian cysts.

Experimental Design: Metabolomic profiling was performed on an initial set of sera from 101 serous and nonserous ovarian cancer cases and 134 individuals with benign pelvic masses (BPM). Using a deep learning model, a panel consisting of seven cancer-related metabolites [diacetylspermine, diacetylspermidine, N-(3-acetamidopropyl)pyrrolidin-2-one, N-acetylneuraminate, N-acetyl-mannosamine, N-acetyl-lactosamine, and hydroxyisobutyric acid] was developed for distinguishing early-stage ovarian cancer from BPM. The performance of the metabolite panel was evaluated in an independent set of sera from 118 ovarian cancer cases and 56 subjects with BPM. The contributions of the panel for improving upon the performance of ROMA were further assessed.

Results: A 7-marker metabolite panel (7MetP) developed in the training set yielded an AUC of 0.86 [95% confidence interval (CI): 0.76–0.95] for early-stage ovarian cancer in the independent test set. The 7MetP+ROMA model had an AUC of 0.93 (95% CI: 0.84–0.98) for early-stage ovarian cancer in the test set, which was improved compared with ROMA alone [0.91 (95% CI: 0.84–0.98); likelihood ratio test *P*: 0.03]. In the entire specimen set, the combined 7MetP+ROMA model yielded a higher positive predictive value (0.68 vs. 0.52; one-sided $P < 0.001$) with improved specificity (0.89 vs. 0.78; one-sided $P < 0.001$) for early-stage ovarian cancer compared with ROMA alone.

Conclusions: A blood-based metabolite panel was developed that demonstrates independent predictive ability and complements ROMA for distinguishing early-stage ovarian cancer from benign disease to better inform clinical decision making.

Introduction

Ovarian cysts are found to occur in some 17% of women who undergo transvaginal sonograms (TVS). Most of these cysts are noncancerous (1, 2). Currently, neither TVS nor cancer antigen 125 (CA125) alone or in combination yield sufficient sensitivity and specificity to distinguish benign form malignant ovarian cysts (3). The high false-positive rates lead to unnecessary surgical procedures, with significant morbidity (4).

Two risk assessment algorithms, the risk of ovarian malignancy algorithm (ROMA) and the risk of ovarian cancer algorithm (OVERA), were developed to assess the risk of a mass being cancerous (5–8). ROMA and OVERA have similar abilities to distinguish malignant from benign pelvic masses (7, 8). Although these algorithms offer high sensitivity for detection of ovarian cancer, specificity is limited (5–8).

Perturbed cellular metabolism is a hallmark of cancer (9). Several lines of evidence indicate that cellular and systemic metabolic adaptations occur from the earliest phases of cancer development, suggesting that metabolites may serve as cancer biomarkers (10, 11). Here, we applied a deep learning approach to metabolic profiles of sera to determine whether a metabolic signature may be uncovered that distinguish early-stage ovarian cancers from benign disease. A model consisting of seven cancer-relevant metabolites, including three polyamines, was developed and tested in an independent set in combination with the ROMA algorithm for ovarian cancer risk prediction among women with ovarian cysts.

Materials and Methods

Specimen sets

Blood specimens were obtained preoperatively with informed consent under Institutional Review Board (IRB)/ethical committees–approved protocols (LAB04-0687) at The University of Texas MD Anderson Cancer Center (MDACC) and at the Fred Hutchinson Cancer Research Center (FHCRC; IRB 4563) from patients who were admitted for surgery based on a mass found on ultrasound, elevated CA125, or a positive biopsy. This study was approved and monitored by the respective IRBs and was conducted in accordance with the Declaration of Helsinki. All human biospecimens were obtained with written informed consent. All patients were fasting at the time of blood collection. Samples were processed on the same day, generally within 4 hours of blood draw, under standardized operating procedures, aliquoted to minimize freeze-thaw cycling effects, and stored in −80°C

[1]Department of Biostatistics, The University of Texas MD Anderson Cancer Center, Houston, Texas. [2]Department of Experimental Therapeutics, The University of Texas MD Anderson Cancer Center, Houston, Texas. [3]Department of Clinical Cancer Prevention, The University of Texas MD Anderson Cancer Center, Houston, Texas. [4]Translational Research Program, Fred Hutchinson Cancer Research Center, Seattle, Washington. [5]Division of Gynecologic Oncology, Swedish Cancer Institute, Seattle, Washington. [6]Department of Gynecological Oncology and Reproductive Medicine, The University of Texas MD Anderson Cancer Center, Houston, Texas.

E. Irajizad and C.Y. Han share co-first authorship of this article.

Corresponding Authors: Johannes F. Fahrmann, Clinical Cancer Prevention, The University of Texas MD Anderson Cancer Center, 6767 Bertner Avenue, Houston, TX 77030. Phone: 713-792-8239; Fax: 713-792-1474; E-mail: jffahrmann@mdanderson.org; and Samir M. Hanash, shanash@mdanderson.org

Clin Cancer Res 2022;28:4669–76

doi: 10.1158/1078-0432.CCR-22-1113

Translational Relevance

Two FDA-approved algorithms, the risk of ovarian malignancy algorithm (ROMA) and the risk of ovarian cancer algorithm (OVERA), have been developed to assess the likelihood of a mass being cancerous. Although these algorithms offer high sensitivity for detection of ovarian cancer, specificity is limited, which can result in high false-positive rates, increased patient anxiety, and unnecessary procedures that are associated with significant morbidity. Here, we developed and independently validated a blood-based metabolite panel for distinguishing early-stage ovarian cancers from benign pelvic masses. We additionally showed that the metabolite panel in combination with ROMA yields a higher positive predictive value with improved specificity for early-stage ovarian cancer compared with ROMA alone. The metabolite panel provides a clinical tool that complements ROMA for improved prediction of malignancy. Such a test would better inform clinical decision making and improve patient outcomes.

until use. The specimen set consisted of plasma from 59 patients with stage I–II and 160 patients with stage III–IV invasive epithelial ovarian cancer and from 190 patients with benign pelvic masses (3, 12). Biopsy samples were examined by a certified pathologist for the diagnosis of cancer or benign pelvic condition. Detailed patient and tumor characteristics are provided in Supplementary **Table S1**. Information regarding histologic ovarian cancer subtypes and benign etiologies are provided in Supplementary Table S1. All participants had provided consent for use of samples in ethically approved secondary studies.

Metabolomic analysis

Metabolomic analyses were performed as described previously (13).

Primary metabolites and biogenic amines

Metabolites were extracted from prealiquoted EDTA plasma (10 μL) with 30 μL of LC/MS grade methanol (Thermo Fisher Scientific) in a 96-well microplate (Eppendorf). Plates were heat sealed, vortexed for 5 minutes at 750 rpm, and centrifuged at 2,000 × *g* for 10 minutes at room temperature. The supernatant (10 μL) was carefully transferred to a 96-well plate, leaving behind the precipitated protein. The supernatant was further diluted with 10 μL of 100 mmol/L ammonium formate, pH3. For hydrophilic interaction liquid chromatography (HILIC) analysis, the samples were diluted with 60 μL LC/MS grade acetonitrile (Thermo Fisher Scientific), whereas samples for C18 analysis were diluted with 60 μL water (GenPure ultrapure water system, Thermo Fisher Scientific). Each sample solution was transferred to 384-well microplate (Eppendorf) for LC/MS analysis.

Untargeted analysis of primary metabolites and biogenic amines

Untargeted metabolomics analysis was conducted on Waters Acquity UPLC system with two-dimensional column regeneration configuration (I-class and H-class) coupled to a Xevo G2-XS quadrupole time-of-flight mass spectrometer. Chromatographic separation was performed using HILIC (Acquity UPLC BEH amide, 100 Å, 1.7 μm 2.1× 100 mm, Waters Corporation) and C18 (Acquity UPLC HSS T3, 100 Å, 1.8 μm, 2.1×100 mm, Water Corporation) columns at 45°C.

Quaternary solvent system mobile phases were (A) 0.1% formic acid in water, (B) 0.1% formic acid in acetonitrile, and (D) 100 mmol/L ammonium formate, pH 3. Samples were separated using the following gradient profile: for the HILIC separation a starting gradient of 95% B and 5% D was increase linearly to 70% A, 25% B, and 5% D over a 5-minute period at 0.4 mL/minute flow rate, followed by 1 minute isocratic gradient at 100% A at 0.4 mL/minute flow rate. For C18 separation, a chromatography gradient of was as follows: starting conditions, 100% A, with linear increase to final conditions of 5% A, 95% B followed by isocratic gradient at 95% B, 5% D for 1 minute.

Binary pump was used for column regeneration and equilibration. The solvent system mobile phases were (A1) 100 mmol/L ammonium formate, pH 3, (A2) 0.1% formic in 2-propanol and (B1) 0.1% formic acid in acetonitrile. The HILIC column was stripped using 90% A2 for 5 minutes followed by 2 minutes equilibration using 100% B1 at 0.3 mL/minute flow rate. Reverse phase C18 column regeneration was performed using 95% A1, 5% B1 for 2 minutes followed by column equilibration using 5% A1, 95% B1 for 5 minutes.

Mass spectrometry data acquisition

Mass spectrometry data were acquired using "sensitivity" mode in positive and negative electrospray ionization mode within 50–1,200 Da range for primary metabolites and 100–2,000 Da for complex lipids. For the electrospray acquisition, the capillary voltage was set at 1.5 kV (positive), 3.0 kV (negative), sample cone voltage 30 V, source temperature at 120°C, cone gas flow 50 L/hour and desolvation gas flow rate of 800 L/hour with scan time of 0.5 seconds in continuum mode. Leucine Enkephalin; 556.2771 Da (positive) and 554.2615 Da (negative) was used for lockspray correction and scans were performed at 0.5 minute. The injection volume for each sample was 3 μL, unless otherwise specified. The acquisition was carried out with instrument auto gain control to optimize instrument sensitivity over the samples acquisition time.

Data processing

Data were processed using Progenesis QI (Nonlinear, Waters). Peak picking and retention time alignment of LC/MS and MSe data were performed using Progenesis QI software (Nonlinear, Waters). Data processing and peak annotations were performed using an in-house automated pipeline as described previously (13–16). Annotations were determined by matching accurate mass and retention times using customized libraries created from authentic standards and by matching experimental tandem mass spectrometry data against the NIST MSMS, LipidBlast, or HMDB v3 theoretical fragmentations; for complex lipids retention time patterns characteristic of lipid subclasses was also considered. To correct for injection order drift, each feature was normalized using data from repeat injections of quality control samples collected every 10 injections throughout the run sequence. Measurement data were smoothed by Locally Weighted Scatterplot Smoothing (LOESS) signal correction (QC-RLSC) as described previously. Values are reported as ratios relative to the median of historical quality control reference samples run with every analytic batch for the given analyte (13–16).

Assaying of CA125 and HE4

Serum CA125 and HE4 concentrations were measured using the Architect CA125II assay (Abbott Diagnostics), and the HE4 EIA assay (Fujirebio Diagnostics) as described previously (17). To calculate the ROMA score, a predictive index (PI) was calculated using serum HE4 and CA125 II levels and one of the following equations, depending on the patient's menopausal status as described previously (7):

Premenopausal: Predictive Index (PI) = −12.0 + 2.38*Natural Log[HE4] + 0.0626*Natural Log[CA 125]
Postmenopausal: Predictive Index (PI) = −8.09 + 1.04*Natural Log[HE4] + 0.732*Natural Log[CA 125]
ROMA percentage were calculated by $\exp(PI)/(1+\exp(PI))$.

Statistical analysis

An overall schematic workflow of the study is provided in Supplementary Fig. S1. Metabolite selection and model building was performed using metabolic profiles generated from plasma samples from the FHCRC. The method reported by Gedeon was used to prioritize pertinent variables to be included in the model (18–20). This approach removes irrelevant or noisy variables by analyzing for the relative weight of each variable within the overall data matrix. An importance score is calculated by dividing the absolute value of the weight of an input connecting to an output by the total absolute value of all weights from that input. When applied in the deep learning model (DLM), this approach is recursively extended backward through layers by taking the effect of a neuron on a connected node, then multiplying the derived weight by the effect of the given node on the target output and summing all connecting nodes.

$$P_{jk} = \frac{|w_{jk}|}{\sum_{r=1}^{nh}|w_{rk}|}$$

Here, P_{jk} represents the average contribution of a node j in a layer to a node k in the next layer. w is the weight on the connection and nh is the number of nodes in the next layer.

The contribution of an input neuron to an output is:

$$Q_{ik} = \sum_{r=1}^{nh}(P_{ir} \times P_{rk})$$

Using this approach, 20 iterations with slightly modified hyperparameters were introduced, and the relative variable importance score recalculated for each metabolite. Metabolites that consistently yielded a relative variable importance score >0.7 (corresponding to those metabolites with importance scores in the top 30th percentile) across all 20 iterations were selected to develop an algorithm for distinguishing early-stage ovarian cancer from benign disease. Seven models, including deep learning, random forest, ensemble learning, and gradient boosting method algorithms, incorporating the seven metabolites were assessed for distinguishing early-stage ovarian cancer from benign disease. Performance of the models was evaluated using a 5-fold cross-validation. To further evaluate model stability, perturbations (e.g., random selection and replacement) were introduced to the training set and the performance reassessed.

A DLM with three hidden layers and three nodes in each layer was selected for modeling the 7-marker metabolite panel (7MetP) based on AUC, and the 7MetP using fixed parameters tested for detection of ovarian cancer in the MDACC cohort.

To assess the contributions of the 7MetP and ROMA, we first fitted a logistic regression with the 7MetP and ROMA as two separate predictors (Supplementary Table S2). For ROMA, we used percentage risk as described above (21). Initial modeling was performed using early-stage ovarian cancer cases and individuals with BPM from the FHCRC and testing of the model performed in the MDACC cohort.

To directly compare the performance of the combined 7MetP+ROMA model with ROMA, we used fixed risk thresholds of 11.4% in premenopausal women and 29.9% for postmenopausal (21), and calculated positive predictive values (PPV), negative predictive values (NPV) as well as sensitivity and specificity estimates.

The combined score from the logistic regression model were converted to risk by $\exp(combined\ score)/(1+\exp(combined\ score))$.

Model discrimination was assessed on the basis of ROC curve, as well as sensitivity and specificity estimates. The 95% confidence intervals (CI) for AUCs were estimated using the Delong method (22). *P* values for specificity and sensitivity were estimated by calculating 2.5 and 97.5 percentiles of 1,000 boot straps on the delta values. All modeling was performed using the *h2o* package and R statistical program (18).

Data availability

Relevant data supporting the findings of this study are available within the article and Supplementary Data or are available from the authors upon reasonable request.

Results

Feature selection for algorithm training

Untargeted metabolomics was conducted on a training set of sera from 101 ovarian cancer cases (39 early stage and 62 late stage) and 134 subjects with BPM from the FHCRC (**Table 1**). A total of 475 uniquely annotated metabolites were quantified (Supplementary Table S3). To prioritize metabolites, relative importance scores were calculated using the Gedeon method (19, 20) and metabolites selected based on consistently exhibiting an importance score above 0.7. This approach resulted in seven metabolites each of which had prior evidence for cancer relevance [diacetylspermine (23), diacetylspermidine (15), N-(3-acetamidopropyl)pyrrolidin-2-one (15), N-acetylneuraminate (NANA; ref. 23), N-acetyl-mannosamine (24), N-acetyl-lactosamine (25), and hydroxyisobutyric acid (26)] that were subsequently used for model building. Individual classifier performance of these metabolites for distinguishing ovarian cancer cases from individuals with BPM ranged from 0.55 to 0.82 (Supplementary Table S4; Supplementary Fig. S2).

Development of a combination rule and validation in an independent test set

We next sought to develop an optimal combination rule that incorporated the seven metabolites for distinguishing early-stage ovarian cancer from benign disease. For model building, we tested seven different machine learning algorithms. Of these, a DLM with three hidden layers and three nodes in each layer achieved the highest predictive performance and was used to establish the 7MetP, which yielded an AUC of 0.75 (95% CI: 0.66–0.85) for differentiating early-stage ovarian cancer cases from benign disease (**Table 2**; Supplementary Tables S5 and S6). When stratifying ovarian cancer cases into serous and nonserous, the 7MetP had respective AUCs of 0.85 (95% CI: 0.79–0.91) and 0.80 (95% CI: 0.71–0.89; Supplementary Table S7).

Validation of the 7MetP using fixed parameters was performed in an independent test set from MDACC that consisted of 118 ovarian cancer cases (20 early stage and 98 late stage) and 56 individuals with BPM. The 7MetP yielded an AUC of 0.88 (95% CI: 0.82–0.93) for distinguishing all ovarian cancer cases from individuals with BPM (Supplementary Table S5), and an AUC of 0.86 (95% CI: 0.76–0.95) for early-stage ovarian cancer (**Fig. 1**; Supplementary Table S5).

Contributions of the metabolite panel with the ROMA algorithm

We next assessed whether the 7MetP would improve upon the predictive performance of the ROMA algorithm. Using model scores

Table 1. Patient and tumor characteristics.

Patient and tumor characteristics	Training set			Testing set		
	Cases	BPM[a]	*P*[b]	Cases	BPM[a]	*P*[b]
Number of subjects, *N*	101	134		118	56	
Age, average (min–max)	59 (23–85)	57 (30–83)	0.14	61 (36–86)	55 (33–79)	0.009
Menopausal status, *N* (%)						
Pre	21 (20.8%)	39 (29.1%)	0.17	19 (16.1%)	18 (32.1%)	0.02
Post	80 (79.2%)	95 (70.9%)		99 (83.8%)	38 (67.8%)	
Race, *N* (%)						
White	83 (82.2%)	104 (77.6%)	0.18	87 (73.7%)	42 (75%)	0.52
Black	5 (5%)	3 (2.2%)		9 (7.6%)	9 (16.1%)	
Asian	2 (2%)	3 (2.2%)		13 (11%)	1 (1.8%)	
American Indian	—	1 (0.7%)		—	—	
Pacific Islander	—	—		9 (7.6%)	4 (7.1%)	
Unknown	11 (10.9%)	23 (17.2%)		—	—	
Stage, *N* (%)						
Stage I and II	39 (38.6%)	—		20 (16.9%)	—	
Stage III and IV	62 (61.4%)	—		98 (83.1%)	—	
Histologic subtype, *N* (%)						
Serous	69 (68.3%)	—		114 (96.6%)	—	
Nonserous	32 (31.7%)	—		1 (0.8%)	—	
Unknown				3 (2.54%)		
ROMA, median (25th/75th percentiles)	86.85 (36.85–98.03)	11.14 (6.64–20.66)	<0.0001	89.51 (70.55–96.95)	13.66 (6.42–18.56)	<0.0001

[a]Individuals with BPM.
[b]Statistical significance was determined by Wilcoxon rank-sum tests for continuous variables and Fisher exact test or χ^2 tests for trend for categorical variables. Two-sided *P* values are reported.

derived from the 7MetP and the ROMA algorithm, a logistic regression model for distinguishing early-stage ovarian cancer from BPM was developed in the training set and performance evaluated in the test set. The combined 7MetP+ROMA yielded an AUC of 0.93 (95% CI: 0.86–1.00) for early-stage ovarian cancer in the test set whereas ROMA alone had an AUC of 0.91 (95% CI: 0.84–0.98; likelihood ratio test *P*: 0.03; **Table 3**). Compared with ROMA, the combined 7MetP+ROMA yielded improvements in the PPV by 21.0% (one-sided $P < 0.001$) and specificity by 14.0% (one-sided $P < 0.001$) for early-stage ovarian cancer (**Table 3**). When considering all ovarian cancer cases, the combined 7MetP+ROMA model yielded an AUC of 0.97 (95% CI: 0.94–0.99) in the test set (**Table 4**).

Performance of the metabolite panel alone and in combination with ROMA in the combined training and test sets

We further evaluated the predictive performance of the 7MetP alone and in combination with ROMA in the entire specimen set [$n = 219$ ovarian cancer cases (59 early stage and 160 late stage and 190 BPM)]. The 7MetP had an AUC of 0.85 (95% CI: 0.81–0.88) for distinguishing all ovarian cancer cases from individuals with BPM and an AUC of

Table 2. Performance of different learning algorithms for differentiating early-stage ovarian cancer cases from BPM in the training set using 5-fold cross-validation.

Model	Hyperparameters	AUC	Log loss	AUCpr	Mean per class error	RMSE
Deep learning model	Activation: MaxoutWithDropout, hidden layers: [3, 3, 3]	0.753	0.354	0.556	0.222	0.303
Deep learning model	Activation: Tanh, hidden layers: [1, 1]	0.740	0.362	0.529	0.233	0.322
StackedEnsemble	Ensemble models: GLM, Deep Learning, Random Forest, Gradient Boost Method	0.713	0.387	0.484	0.205	0.332
Deep learning model	Activation: Tanh, hidden layers: [2, 2]	0.711	0.377	0.519	0.237	0.325
Lasso regression	Lambda = 0.2,5 features selected	0.709	0.506	0.438	0.202	0.376
StackedEnsemble	Ensemble models (best of each family): GLM, Deep Learning, Random Forest, Gradient Boost Method	0.692	0.399	0.459	0.228	0.336
GLM	Family: binomial	0.687	0.532	0.447	0.241	0.364
Extremely randomized trees (XRT)	—	0.681	0.577	0.359	0.224	0.351
Distributed random forest (DRF)	—	0.679	0.746	0.355	0.216	0.354
Gradient boosting method	Number of tree: 50, Maximum depth: 6	0.668	0.516	0.357	0.234	0.372

Abbreviations: AUC, area under the ROC curve; AUCpr, area under the precision recall curve; RMSE, root-mean-square deviation.

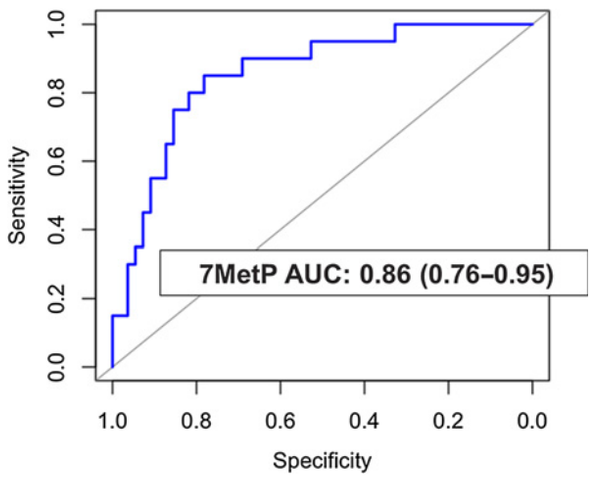

Figure 1.
Predictive performance of the 7MetP for distinguishing early-stage ovarian cancer from BPM in the independent test set.

0.81 (95% CI: 0.76–0.86) for early-stage ovarian cancer (Supplementary Table S5). The combined 7MetP+ROMA model had a resultant AUC of 0.87 (95% CI: 0.85–0.93) for early-stage ovarian cancer, which was markedly improved compared with ROMA alone [AUC: 0.84 (95% CI: 0.81–0.90); likelihood ratio test *P*: < 0.001] (**Table 5**; Supplementary Table S8). Importantly, compared with ROMA alone, the 7MetP+ROMA model yielded a statistically significantly (one-sided $P < 0.001$) higher PPV (0.68 vs. 0.52) and specificity (0.89 vs. 0.78) for early-stage ovarian cancer (**Table 5**).

Discussion

Pelvic masses are relatively common among women of all ages, usually necessitating surgery. However, most such masses are benign and only a small percentage of these women will be diagnosed with ovarian cancer (27).

Algorithms such as OVERA and ROMA were developed to estimate probability of a woman with a pelvic mass harboring a malignancy and to determine whether a patient should be referred to a general gynecologist if the mass is likely to be benign or a gynecologic oncologist if the mass is likely to be malignant (7, 28, 29). A gynecologic oncologist has specialized training to dissect nodes, remove the omentum, and to remove as much cancer as possible from the surface of the bowel if extensive disease is found. Although the OVERA and ROMA algorithms offer high sensitivity, they are limited by suboptimal specificity which can result in high false-positive rates, increased patient anxiety, and unnecessary procedures that are associated with significant morbidity (30, 31). A test that offers high sensitivity and specificity for identifying individuals at high risk of harboring malignant ovarian cysts has potential to better inform clinical decision making and improve patient outcomes. We developed and validated a blood-based metabolite panel that improves prediction of malignancy in combination with ROMA for women presenting with ovarian cysts.

The metabolite panel includes three polyamines, three acetylated carbohydrates, and hydroxyisobutyric acid. We have previously shown utility of circulating polyamines for early detection of ovarian cancer (15). Polyamines have also been reported to be elevated in urine of individuals with ovarian cancer compared with controls (32). The acetylated carbohydrates NANA and NAMA are involved in metabolism of sialic acids, which are commonly found in glycans of cell surface glycoproteins and glycolipids. Sialic acids are known to be involved in various aspects of tumorigenesis, including promoting tumor growth and metastasis as well as immune evasion (33–36). Moreover, sialic acids can accumulate in the circulation due to increased turnover, secretion, and/or shedding (37). N-acetyllactosamine is a reported carbohydrate antigen involved in malignant transformation and metastasis (25, 38, 39). Hydroxyisobutyric acid, a metabolite derived from valine metabolism, has also been linked to cancer with diagnostic and prognostic applications in ovarian cancer (26).

Table 3. Performance estimates of ROMA and the combined 7MetP+ROMA model for early-stage ovarian cancer the training set and the independent testing set.

		Training set			
		ROMA	**ROMA + 7MetP**	**Difference**	***P***
	AUC (95% CI)	0.81 (0.77–0.85)	0.84 (0.80–0.88)	0.03 (0.01 to 0.06)	<**0.001**
At 11.4% risk threshold for premenopausal and 29.9% for postmenopausal (same risk as ROMA)	Sensitivity	0.68 (0.60–0.77)	0.68 (0.59–0.77)	0.00 (−0.06 to 0.07)	0.49
	Specificity	0.79 (0.75–0.83)	0.88 (0.85–0.91)	0.09 (0.06 to 0.12)	<**0.001**
	PPV	0.48 (0.40–0.55)	0.62 (0.54–0.69)	0.14 (0.08 to 0.20)	<**0.001**
	NPV	0.90 (0.87–0.93)	0.91 (0.88–0.94)	0.01 (−0.01 to 0.03)	0.14
		Test set			
		ROMA	**ROMA + 7MetP**	**Difference**	***P***
	AUC (95% CI)	0.91 (0.84–0.98)	0.93 (0.86–1.00)	0.02 (−0.01 to 0.04)	**0.03**
At 11.4% risk threshold for premenopausal and 29.9% for postmenopausal (same risk as ROMA)	Sensitivity	0.90 (0.83–0.97)	0.90 (0.81–0.97)	0.00 (−0.09 to 0.09)	0.472
	Specificity	0.77 (0.70–0.83)	0.91 (0.86–0.95)	0.14 (0.09 to 0.20)	<**0.001**
	PPV	0.58 (0.48–0.68)	0.79 (0.67–0.87)	0.21 (0.13 to 0.28)	<**0.001**
	NPV	0.96 (0.92–0.99)	0.96 (0.93–0.99)	0.01 (−0.03 to 0.04)	0.365

Note: *P* values for comparison of AUCs represent likelihood ratio tests. Risk threshold corresponding to 11.4% in premenopausal women and 29.9% for postmenopausal were chosen based on reported findings from Ortiz-Munoz and colleagues (21). One-sided *P* values are reported as we expect that the combined 7MetP+ROMA will yield improved performance estimates compared with ROMA alone.
Abbreviations: NPV, negative predictive value; PPV, positive predictive value.

Table 4. Performance estimates of ROMA and the combined 7MetP+ROMA model for all ovarian cancer in the training set and the independent testing set.

		Training set			
		ROMA	**ROMA + 7MetP**	**Difference**	***P***
	AUC (95% CI)	0.91 (0.89–0.93)	0.93 (0.91–0.94)	0.01 (0.00 to 0.03)	<**0.001**
At 11.4% risk threshold for premenopausal and 29.9% for postmenopausal (same risk as ROMA)	Sensitivity	0.87 (0.83–0.91)	0.86 (0.82–0.90)	−0.01 (−0.04 to 0.02)	0.22
	Specificity	0.79 (0.75–0.83)	0.88 (0.85–0.91)	0.09 (0.06 to 0.12)	<**0.001**
	PPV	0.76 (0.71–0.80)	0.84 (0.81–0.89)	0.09 (0.05 to 0.12)	<**0.001**
	NPV	0.89 (0.86–0.92)	0.89 (0.86–0.92)	0.00 (−0.02 to 0.02)	0.36
		Test set			
		ROMA	**ROMA + 7MetP**	**Difference**	***P***
	AUC (95% CI)	0.96 (0.94–0.99)	0.97 (0.94–0.99)	0.01 (0.00 to 0.01)	0.06
At 11.4% risk threshold for premenopausal and 29.9% for postmenopausal (same risk as ROMA)	Sensitivity	0.96 (0.93–0.98)	0.93 (0.90–0.96)	−0.03 (−0.05 to −0.01)	**0.008**
	Specificity	0.76 (0.70–0.83)	0.91 (0.86–0.95)	0.15 (0.10 to 0.20)	<**0.001**
	PPV	0.89 (0.86–0.93)	0.96 (0.93–0.97)	0.06 (0.04 to 0.09)	<**0.001**
	NPV	0.89 (0.84–0.94)	0.86 (0.81–0.91)	−0.03 (−0.08 to 0.01)	0.07

Note: *P* values for comparison of AUCs represent likelihood ratio tests. Risk threshold corresponding to 11.4% in premenopausal women and 29.9% for postmenopausal were chosen based on reported findings from Ortiz-Munoz and colleagues (21). One-sided *P* values are reported as we expect that the combined 7MetP+ROMA will yield improved performance estimates compared to ROMA alone.
Abbreviations: NPV, negative predictive value; PPV, positive predictive value.

Table 5. Performance estimates of ROMA and the combined 7MetP+ROMA model for early-stage ovarian cancer in the combined specimen set.

		Entire set			
		ROMA	**ROMA + 7MetP**	**Difference**	***P***
	AUC (95% CI)	0.84 (0.79–0.90)	0.87 (0.82–0.93)	0.03 (0.01 to 0.04)	<**0.001**
At 11.4% risk threshold for premenopausal and 29.9% for postmenopausal (same risk as ROMA)	Sensitivity	0.76 (0.69–0.82)	0.76 (0.70–0.82)	0.00 (−0.04 to 0.05)	0.464
	Specificity	0.78 (0.75–0.81)	0.89 (0.86–0.92)	0.11 (0.08 to 0.14)	<**0.001**
	PPV	0.52 (0.45–0.58)	0.68 (0.61–0.75)	0.16 (0.11 to 0.21)	<**0.001**
	NPV	0.91 (0.89–0.94)	0.92 (0.90–0.94)	0.01 (−0.01 to 0.02)	0.091

Note: *P* values for comparison of AUCs represent likelihood ratio tests. Risk threshold corresponding to 11.4% in premenopausal women and 29.9% for postmenopausal were chosen based on reported findings from Ortiz-Munoz and colleagues (21). One-sided *P* values are reported as we expect that the combined 7MetP+ROMA will yield improved performance estimates compared with ROMA alone.
Abbreviations: NPV: negative predictive value; PPV: positive predictive value.

On balance, limitations to our study including the unbalanced distribution of histology across the test and validation sets. Ovarian cancer cases were largely at advanced stages of disease in the specimen sets with differential representation of nonserous and serous ovarian cancer. The metabolite panel yielded comparable performance for distinguishing serous and nonserous ovarian cancer from BPM. Moreover, our metabolite panel was developed using early-stage ovarian cancer cases and validated in an independent set of early-stage ovarian cancer cases. Contributions of the metabolite panel with the OVERA algorithm were not assessed. Comparison of performance estimates between ROMA and OVERA has shown that they are comparable with tradeoffs in sensitivity and specificity (7, 40, 41). Although PPV and NPV estimates are dependent upon the prevalence of disease in the evaluated population, previous investigations have reported ROMA to have a PPV of 42.9% (7), which is consistent with our findings. OVERA has a reported PPV of 40% (8). In our study, the 7MetP+ROMA model had PPV of 68.0%. Thus, we believe that the metabolite panel has the potential to significantly contribute to the OVERA as well.

In conclusion, we developed and validated a metabolite panel that complements ROMA for improved risk prediction of malignancy among women presenting with ovarian cysts.

Authors' Disclosures

E. Irajizad reports a patent for METHODS FOR THE DETECTION AND TREATMENT OF OVARIAN CANCER (MDA0071-101) pending. R. Wu reports a patent for MDA0071-101 pending. E. Murage reports a patent for METHODS FOR THE DETECTION AND TREATMENT OF OVARIAN CANCER (MDA0071-101) pending. R. Spencer reports a patent for MDA0071-101 pending. J.B. Dennison reports a patent for METHODS FOR THE DETECTION AND TREATMENT OF OVARIAN CANCER (MDA0071-101) pending. J.P. Long reports grants from NIH during the conduct of the study; grants from NIH outside the submitted work. R.C. Bast reports personal fees from Fujirebio Diagnostics Inc during the conduct of the study. S. Hanash reports a patent for METHODS FOR THE DETECTION AND TREATMENT OF OVARIAN CANCER pending. J.F. Fahrmann reports a patent for METHODS FOR THE DETECTION AND TREATMENT OF OVARIAN CANCER pending. No disclosures were reported by the other authors.

Authors' Contributions

E. Irajizad: Conceptualization, data curation, formal analysis, validation, investigation, visualization, methodology, writing–original draft. **C.Y. Han:** Resources, writing–review and editing. **J. Celestino:** Resources, writing–review and editing. **R. Wu:** Methodology, writing–review and editing. **E. Murage:** Data curation, methodology, writing–review and editing. **R. Spencer:** Resources, writing–review and editing. **J.B. Dennison:** Methodology, project administration, writing–review and editing. **J. Vykoukal:** Writing-review and editing. **J.P. Long:** Formal analysis,

funding acquisition, writing–review and editing. **K.A. Do:** Formal analysis, funding acquisition, writing–review and editing. **C. Drescher:** Resources, writing–review and editing. **K. Lu:** Resources, writing–review and editing. **Z. Lu:** Resources, writing–review and editing. **R.C. Bast:** Resources, funding acquisition, writing–review and editing. **S. Hanash:** Conceptualization, resources, formal analysis, supervision, project administration, writing–review and editing. **J.F. Fahrmann:** Conceptualization, data curation, formal analysis, supervision, validation, investigation, visualization, methodology, writing–original draft, project administration.

Acknowledgments

Supported in part through the Cancer Prevention and Research Institute of Texas grants RP160145 and RP101382, the generous philanthropic contributions to The University of Texas MD Anderson Cancer Center Moon Shots Program and a faculty fellowship from The University of Texas MD Anderson Cancer Center Duncan Family Institute for Cancer Prevention and Risk Assessment (J.F. Fahrmann). This work was also supported by grants from the NCI Early Detection Research Network (5 U01 CA200462-02), the MD Anderson Ovarian SPORE (P50 CA217685), NCI, Department of Health and Human Services; the Cancer Prevention Research Institute of Texas (RP160145); Golfers Against Cancer, Ann and Henry Zarrow Foundation; the Mossy Foundation, the Roberson Endowment, and generous donations from Stuart and Gaye Lynn Zarrow, Barry Elson, and Arthur and Sandra Williams. K.A. Do was partially supported by NIH SPORE grant P50CA140388, CCTS grant 5UL1TR0003167, CPRIT grant RP160693, and the NCI grant CA016672.

The publication costs of this article were defrayed in part by the payment of publication fees. Therefore, and solely to indicate this fact, this article is hereby marked "advertisement" in accordance with 18 USC section 1734.

Note

Supplementary data for this article are available at Clinical Cancer Research Online (http://clincancerres.aacrjournals.org/).

Received April 6, 2022; revised June 6, 2022; accepted August 24, 2022; published first August 29, 2022.

References

1. Buys SS, Partridge E, Greene MH, Prorok PC, Reding D, Riley TL, et al. Ovarian cancer screening in the prostate, lung, colorectal and ovarian (PLCO) cancer screening trial: findings from the initial screen of a randomized trial. Am J Obstet Gynecol 2005;193:1630–9.
2. Pavlik EJ, Ueland FR, Miller RW, Ubellacker JM, DeSimone CP, Elder J, et al. Frequency and disposition of ovarian abnormalities followed with serial transvaginal ultrasonography. Obstet Gynecol 2013;122:210–7.
3. Lu KH, Skates S, Hernandez MA, Bedi D, Bevers T, Leeds L, et al. A 2-stage ovarian cancer screening strategy using the risk of ovarian cancer algorithm (ROCA) identifies early-stage incident cancers and demonstrates high positive predictive value. Cancer 2013;119:3454–61.
4. Buys SS, Partridge E, Black A, Johnson CC, Lamerato L, Isaacs C, et al. Effect of screening on ovarian cancer mortality: the prostate, lung, colorectal and ovarian (PLCO) cancer screening randomized controlled trial. JAMA 2011;305:2295–303.
5. Dochez V, Caillon H, Vaucel E, Dimet J, Winer N, Ducarme G. Biomarkers and algorithms for diagnosis of ovarian cancer: CA125, HE4, RMI and ROMA, a review. J Ovarian Res 2019;12:28.
6. Ueland FR, Desimone CP, Seamon LG, Miller RA, Goodrich S, Podzielinski I, et al. Effectiveness of a multivariate index assay in the preoperative assessment of ovarian tumors. Obstet Gynecol 2011;117:1289–97.
7. Moore RG, McMeekin DS, Brown AK, DiSilvestro P, Miller MC, Allard WJ, et al. A novel multiple marker bioassay utilizing HE4 and CA125 for the prediction of ovarian cancer in patients with a pelvic mass. Gynecol Oncol 2009;112:40–6.
8. Coleman RL, Herzog TJ, Chan DW, Munroe DG, Pappas TC, Smith A, et al. Validation of a second-generation multivariate index assay for malignancy risk of adnexal masses. Am J Obstet Gynecol 2016;215:82.
9. Pavlova NN, Thompson CB. The emerging hallmarks of cancer metabolism. Cell Metab 2016;23:27–47.
10. Faubert B, Solmonson A, DeBerardinis RJ. Metabolic reprogramming and cancer progression. Science 2020;368:eaaw5473.
11. Boroughs LK, DeBerardinis RJ. Metabolic pathways promoting cancer cell survival and growth. Nat Cell Biol 2015;17:351–9.
12. Yang WL, Gentry-Maharaj A, Simmons A, Ryan A, Fourkala EO, Lu Z, et al. Elevation of TP53 autoantibody before CA125 in preclinical invasive epithelial ovarian cancer. Clin Cancer Res 2017;23:5912–22.
13. Fahrmann JF, Vykoukal J, Fleury A, Tripathi S, Dennison JB, Murage E, et al. Association between plasma diacetylspermine and tumor spermine synthase with outcome in triple-negative breast cancer. J Natl Cancer Inst 2020;112:607–16.
14. Fahrmann JF, Bantis LE, Capello M, Scelo G, Dennison JB, Patel N, et al. A Plasma-derived protein-metabolite multiplexed panel for early-stage pancreatic cancer. J Natl Cancer Inst 2019;111:372–9.
15. Fahrmann JF, Irajizad E, Kobayashi M, Vykoukal J, Dennison JB, Murage E, et al. A MYC-driven plasma polyamine signature for early detection of ovarian cancer. Cancers 2021;13:913.
16. Vykoukal J, Fahrmann JF, Gregg JR, Tang Z, Basourakos S, Irajizad E, et al. Caveolin-1-mediated sphingolipid oncometabolism underlies a metabolic vulnerability of prostate cancer. Nat Commun 2020;11:4279.
17. Yang WL, Lu Z, Guo J, Fellman BM, Ning J, Lu KH, et al. Human epididymis protein 4 antigen-autoantibody complexes complement cancer antigen 125 for detecting early-stage ovarian cancer. Cancer 2020;126:725–36.
18. Candel A, Parmar V, LeDell E, Arora A. Deep learning with H2O. Mountain View, CA: H2O ai Inc; 2016. p. 1–21.
19. Greenwell BM, Boehmke BC, McCarthy AJ. A simple and effective model-based variable importance measure. arXiv preprint arXiv:180504755 2018.
20. Gedeon TD. Data mining of inputs: analysing magnitude and functional measures. Int J Neural Syst 1997;8:209–18.
21. Ortiz-Muñoz B, Aznar-Oroval E, García AG, Peris AC, Ballestero PP, Yepes MS, et al. HE4, Ca125 and ROMA algorithm for differential diagnosis between benign gynaecological diseases and ovarian cancer. Tumor Biol 2014;35:7249–58.
22. DeLong ER, DeLong DM, Clarke-Pearson DL. Comparing the areas under two or more correlated receiver operating characteristic curves: a nonparametric approach. Biometrics 1988;44:837–45.
23. Vimr ER, Troy FA. Regulation of sialic acid metabolism in Escherichia coli: role of N-acylneuraminate pyruvate-lyase. J Bacteriol 1985;164:854–60.
24. Brigham C, Caughlan R, Gallegos R, Dallas MB, Godoy VG, Malamy MH. Sialic acid (N-acetyl neuraminic acid) utilization by Bacteroides fragilis requires a novel N-acetyl mannosamine epimerase. J Bacteriol 2009;191:3629–38.
25. Kadirvelraj R, Yang J-Y, Kim HW, Sanders JH, Moremen KW, Wood ZA. Comparison of human poly-N-acetyl-lactosamine synthase structure with GT-A fold glycosyltransferases supports a modular assembly of catalytic subsites. J Biol Chem 2021;296:100110.
26. Hilvo M, De Santiago I, Gopalacharyulu P, Schmitt WD, Budczies J, Kuhberg M, et al. Accumulated metabolites of hydroxybutyric acid serve as diagnostic and prognostic biomarkers of ovarian high-grade serous carcinomas. Cancer Res 2016;76:796–804.
27. Curtin JP. Management of the adnexal mass. Gynecol Oncol 1994;55:S42–6.
28. Coulter M, Morell A, Samborski A, Miller M, Moore R. Risk of ovarian malignancy algorithm (ROMA) through time and space: a meta-analysis. Gynecol Oncol 2021;162:S266.
29. Carney ME, Lancaster JM, Ford C, Tsodikov A, Wiggins CL. A population-based study of patterns of care for ovarian cancer: who is seen by a gynecologic oncologist and who is not? Gynecol Oncol 2002;84:36–42.
30. Bast RC Jr, Klug TL, John ES, Jenison E, Niloff JM, Lazarus H, et al. A radioimmunoassay using a monoclonal antibody to monitor the course of epithelial ovarian cancer. N Engl J Med 1983;309:883–7.
31. Jacobs I, Bast RC Jr. The CA 125 tumour-associated antigen: a review of the literature. Hum Reprod 1989;4:1–12.
32. Niemi RJ, Roine AN, Hakkinen MR, Kumpulainen PS, Keinanen TA, Vepsalainen JJ, et al. Urinary polyamines as biomarkers for ovarian cancer. Int J Gynecol Cancer 2017;27:1360–6.

33. Munkley J, Scott E. Targeting aberrant sialylation to treat cancer. Medicines 2019;6:102.
34. Büll C, Boltje TJ, Balneger N, Weischer SM, Wassink M, van Gemst JJ, et al. Sialic acid blockade suppresses tumor growth by enhancing T-cell-mediated tumor immunity. Cancer Res 2018;78:3574–88.
35. Dobie C, Skropeta D. Insights into the role of sialylation in cancer progression and metastasis. Br J Cancer 2021;124:76–90.
36. Sun H, Zhou Y, Jiang H, Xu Y. Elucidation of functional roles of Sialic acids in cancer migration. Front Oncol 2020;10:401.
37. Zhang Z, Wuhrer M, Holst S. Serum sialylation changes in cancer. Glycoconj J 2018;35:139–60.
38. Venkitachalam S, Revoredo L, Varadan V, Fecteau RE, Ravi L, Lutterbaugh J, et al. Biochemical and functional characterization of glycosylation-associated mutational landscapes in colon cancer. Sci Rep 2016;6:23642.
39. Qiu H, Duan W-M, Shu J, Cheng H-X, Wang W-P, Huang X-E, et al. B3GNT2, a polylactosamine synthase, regulates glycosylation of EGFR in H7721 human hepatocellular carcinoma cells. Asian Pac J Cancer Prev 2015;15:10875–8.
40. Bristow RE, Smith A, Zhang Z, Chan DW, Crutcher G, Fung ET, et al. Ovarian malignancy risk stratification of the adnexal mass using a multivariate index assay. Gynecol Oncol 2013;128:252–9.
41. Ueland FR. A perspective on ovarian cancer biomarkers: past, present and yet-to-come. Diagnostics 2017;7:14.